Activity, stability and deactivation behavior of Au/CeO$_2$ catalysts in the water gas shift reaction at increased reaction temperature (300 °C)

A. Abd El-Moemen [1], A. Karpenko, Y. Denkwitz, R.J. Behm *

Institute of Surface Chemistry and Catalysis, Ulm University, D-89069 Ulm, Germany

ABSTRACT

The effect of increasing the reaction temperature to 300 °C on the activity, stability and deactivation behavior of a 4.5 wt.% Au/CeO$_2$ catalyst in the water gas shift (WGS) reaction in idealized reformate was studied by kinetic and spectroscopic measurements at 300 °C and comparison with previously reported data for reaction at 180 °C under similar reaction conditions [A. Karpenko, Y. Denkwitz, V. Plzak, J. Cai, R. Leppelt, B. Schumacher, R.J. Behm, Catal. Lett. 116 (2007) 105]. Different procedures for catalyst pretreatment were used, including annealing at 400 °C in oxidative, reductive or inert atmospheres as well as redox processing. The formation/removal of stable adsorbed reaction intermediates and side products (surface carbonates, formates, OH$_{ad}$, CO$_{ad}$) was followed by *in situ* IR spectroscopy (DRIFTS), the presence of differently oxidized surface species (Au^0, Au$^{0'}$, Au^{3+}, Ce^{3+}) was evaluated by XPS. The reaction characteristics at 300 °C generally resemble those at 180 °C, including (i) significantly higher reaction rates, (ii) comparable apparent activation energies ($44 \pm 1/50 \pm 1$ kJ mol^{-1} vs. 40 ± 1 kJ mol^{-1} at 180 °C), (iii) a correlation between deactivation of the catalyst and the build-up of stable surface carbonates, and (iv) a decrease of the initially significant differences in activity after different pretreatment procedures with reaction time. Different than expected, the tendency for deactivation did not decrease with higher temperature, due to enhanced carbonate decomposition, but increases.

© 2008 Elsevier B.V. All rights reserved.

1. Introduction

Recently, the water gas shift (WGS) reaction has attracted increasing interest because of its potential application in fuel cell technology, for the removal of CO from H$_2$-rich feed gases for Polymer Electrolyte Fuel Cells (PEFCs) which are produced, e.g., by steam reforming of organic fuels such as hydrocarbons or methanol [1]. CO acts as a poison for fuel cell anode catalysts, and its concentration has to be reduced to about 10–50 ppm to avoid efficiency losses [1–4]. Industrially, the WGS reaction is carried out in two temperature ranges: (i) as 'high-temperature' shift reaction (320–450 °C) using Fe$_2$O$_3$-Cr$_2$O$_3$ catalysts to obtain high rates, and (ii) as 'low-temperature' shift reaction (200–250 °C) using copper based catalysts for further lowering the CO content [5].

WGS catalysts based on ceria have been investigated in the recent years as alternatives to Cu-ZnO catalyst for applications for fuel processing [6–8]. Ceria is known as an oxygen-storage material, and Luo et al. found a direct relationship between the

WGS activity and the oxygen storage capacity (OSC) [9]. Especially Au/CeO$_2$ catalysts have turned out as very active catalysts for the low-temperature WGS reaction [10–21]. Because of their high low-temperature activity, these catalyst can be operated at even lower temperatures, which would further reduce the steady-state CO content in thermodynamic equilibrium [5]. The technical application of Au/CeO$_2$ catalysts for these purposes is hindered, however, by their strong tendency for deactivation during the reaction. In recent studies from our group as well as from other groups it was demonstrated that the deactivation is closely related to the build-up of stable monodentate carbonate species rather than arising from an irreversible sintering of the Au nanoparticles [15,19,22,23]. These surface carbonates may either directly block active reaction sites or the access of reaction intermediates to the active sites [15,17]. Furthermore, we could demonstrate that high temperature annealing in reactive gases such as H$_2$O or O$_2$ (400 °C) can at least temporarily reduce the deactivation and restore the initial activity [19]. This was correlated with the almost complete removal of the monodentate carbonate species, further supporting the above assignment of surface carbonate accumulation as the origin for deactivation. Under these conditions, it would be tempting to see whether the steady-state concentration of surface carbonates on the Au/CeO$_2$ catalysts and thus the deactivation of the catalyst during the WGS reaction could be reduced by using higher reaction temperatures.

* Corresponding author. Tel.: +49 731 50 25451; fax: +49 731 50 25452.
  E-mail address: juergen.behm@uni-ulm.de (R.J. Behm).
[1] permanent address: Chemistry Department, Faculty of Science, Suez Canal University, Ismailia, Egypt.

Because of the large differences in reaction conditions and catalyst properties in previous studies, it is essentially impossible to answer this question by comparing existing results on the WGS reaction on Au/CeO$_2$ catalysts.

In this paper, we report results of a study on the activity, stability and deactivation behavior of Au/CeO$_2$ catalysts for the WGS reaction at 300 °C reaction temperature, as compared to the previously used 180 °C [15–21]. Since in these previous studies we found that the pretreatment of the catalysts prior to the reaction has considerable effects not only on the activity of the catalyst, but also on its stability and deactivation behavior [16], different catalyst pretreatment procedures were employed. These included oxidative, reductive or redox treatment as well as thermal treatment in inert atmosphere at 400 °C. Because of the higher reaction temperature compared to our previous studies, pretreatment at lower temperatures (200 and 300 °C) was not considered, since after such pretreatments the catalysts are expected to change significantly during the subsequent reaction. The surface composition before and after the WGS reaction was evaluated by X-ray photoelectron spectroscopy (XPS). The formation of reaction intermediates and side products such as formates and carbonates during the reaction was followed by *in situ* diffuse reflectance infrared Fourier transform spectroscopy (DRIFTS). Comparing these data with similar results for a lower reaction temperature (180 °C) shall gain further information on the reaction and deactivation mechanism. Finally, following previous strategies [19,23,24], we explored the effect of a subsequent reactivation treatment, after 1000 min reaction and deactivation, on the catalyst activity and on its surface composition. In addition to revealing possible strategies for reactivation, this may provide additional information on the origin of the observed deactivation. Similar to the deactivation measurements, variations in the surface and adlayer composition were followed by *ex situ* XPS and *in situ* DRIFTS.

2. Experimental

2.1. Catalyst preparation

The catalyst was prepared by a deposition–precipitation procedure, using CeO$_2$ powder as support (HSA 15 from Rhodia, calcined in air at 400 °C) and HAuCl$_4$·4H$_2$O for deposition of Au. Further details are given in refs. [21,25]. The Au metal loading was determined via inductively coupled plasma atom emission spectroscopy (ICP-AES). All measurements were performed with catalysts having a BET surface of 188 m^2 g^{-1} and 4.5 wt.% Au loading. Before the experiments, the catalyst was first heated in N$_2$ to 400 °C, followed by conditioning in different atmospheres at 400 °C for 30 min and finally cooled down in N$_2$ to the reaction temperature. For conditioning, the catalysts were pretreated by different procedures, including (i) calcination in 10% O$_2$, rest N$_2$ (O400), (ii) drying in inert N$_2$ atmosphere (N400), (iii) reduction in 10% H$_2$, rest N$_2$ (H400) or (iv) in 2% CO, N$_2$ (CO400) as well as redox pretreatments, where the catalyst was (v) first conditioned for 30 min in 10% H$_2$, rest N$_2$, then 30 min in 10% O$_2$, rest N$_2$ (H400/O400) and (vi) first calcined for 30 min in 10% O$_2$, N$_2$ then 30 min in 10% H$_2$, rest N$_2$ (O400/H400).

2.2. Catalyst characterization

The chemical composition of the catalyst surface was characterized by XPS (PHI 5800 ESCA system), using monochromatized Al Kα radiation. Survey spectra were measured in the range between 0 and 1400 eV binding energy (BE). Detail spectra of gold (Au(4f)) and cerium (Ce(3d)) were measured in the range from 75 to 100 eV and from 875 to 925 eV (0.125 eV and 20 ms per step), respectively.

Background subtraction and peak fitting were performed using a public XPS peak fit program (XPSPEAK 4.1 by R. Kwok). In order to remove surface charging effects, the BEs were calibrated using the Ce^{4+} (3d^{10}4f^{0}V^n) signal at 916.6 eV as reference [21,26]. The Au(4f) peaks were fitted based on the following assumptions: (i) the difference between Au(4f$_{7/2}$) and Au(4f$_{5/2}$) was fixed at 3.7 eV, (ii) the integral intensity of the Au(4f$_{5/2}$) is three fourth of that of the Au(4f$_{7/2}$) peak and (iii) the peak widths (FWHM) for both peaks are equal [27]. For XPS measurements, catalyst conditioning was performed *ex situ*.

2.3. Activity measurements

Activity measurements were performed in a quartz tube micro reactor (i.d. 4 mm) located in a ceramic tube furnace at atmospheric pressure with typically 60–75 mg diluted catalyst powder. In order to obtain differential reaction conditions (conversion between 5 and 20%), the catalyst was diluted with α-Al$_2$O$_3$, which is not active for the WGS reaction under the present conditions. All reaction measurements were carried out in idealized reformate (1% CO, balance N$_2$ (dry), 2% H$_2$O, 60 N ml min^{-1}) at 300 °C. Water was added to the gas stream using a saturation unit. The incoming and effluent gas flows were analyzed by on-line gas chromatography (Chrompack CP9001) using H$_2$ as a carrier gas. High purity gases from Westphalen (CO 4.7, N$_2$ 6.0, H$_2$ 5.0) were used. Further details on the kinetic measurements are given in ref. [28].

2.4. Infrared measurements

In situ IR investigations were performed in a diffuse reflectance infrared Fourier transform spectroscopy (DRIFTS) configuration with a Magna 560 spectrometer from Nicolet, equipped with a liquid N$_2$ cooled MCT narrow band detector and a commercial *in situ* reaction cell from Harricks (HV-DR2). Gas mixing was performed in the same way as for the activity measurements, with a total flow rate of 60 N ml min^{-1}. Typically, 400 scans (acquisition time 3 min) at a nominal resolution of 8 cm^{-1} were added for one spectrum. The intensities were evaluated in Kubelka–Munk units, which are linearly related to the adsorbate concentration on the catalyst surface [29] (for exceptions see ref. [30]). Normalization and background subtraction of the spectra were performed by comparison with spectra recorded in a flow of 20 N ml N$_2$ (N$_2$-spectra) at the reaction temperature, directly after catalyst conditioning. The spectra recorded during reaction were first normalized to the same background intensity as that of the N$_2$-spectra, and then the latter ones were subtracted from the reaction spectra. If the general shape of the spectra changed during the reaction, normalization to similar backgrounds was made using background intensities close to the respective signal.

3. Results and discussion

3.1. Activity measurements and activation energy

First, we investigated the activity and stability of the 4.5 wt.% Au/CeO$_2$ catalyst during 1000 min WGS reaction in idealized reformate (1% CO, 2% H$_2$O balance N$_2$) at 300 °C after the different pretreatment procedures described in Section 2. The resulting initial and final reaction rates, which differ significantly for the various pretreatments, are listed in Table 1. The deactivation behavior with time is illustrated in Fig. 1a.

The activities are significantly higher than those reported in previous studies for reaction at 180 °C [15,16,19,21], e.g., by about a factor of 2.1 for O400 and 1.3 for H400 pretreatment. Interestingly, the catalysts deactivate in a similar way at the higher

Table 1
Reaction rates during WGS reaction at 300 °C and activation energies in idealized reformate on differently pretreated 4.5 wt.% Au/CeO_2 catalysts

Catalyst pretreatment	Initial rate (mol g_{Au}^{-1} s^{-1})	Rate after 1000 min (mol g_{Au}^{-1} s^{-1})	Relative rate after 1000 min (%)	Activation energy (kJ mol^{-1})
O400	2.3×10^{-3}	6.3×10^{-4}	27	44 ± 2
H400/O400	1.3×10^{-3}	4.7×10^{-4}	36	45 ± 2
N400	8.7×10^{-4}	4.3×10^{-4}	50	46 ± 2
CO 400	7.2×10^{-4}	3.8×10^{-4}	52	45 ± 1
O400/H400	4.2×10^{-4}	2.4×10^{-4}	57	50 ± 1
H400	3.4×10^{-4}	1.9×10^{-4}	57	51 ± 1

reaction temperature as at 180 °C reaction temperature [15,16], at least on a qualitative scale (largely exponential decay, with a steeper decay in the beginning). Both on an absolute and on a relative scale, however, the deactivation is more pronounced at the higher reaction temperature than at the lower temperatures. Hence, the hope that higher reaction temperature would significantly reduce the deactivation is not fulfilled. Similar to reaction at 180 °C, the catalyst pretreatment has considerable influence on its activity and stability. After calcination at 400 °C, the initial and the steady-state activity are highest; they decrease in the order O400 > H400/O400 > N400 > CO400 > O400/H400 > H400. The long-time stability of the catalysts follows the reverse order (see Table 1). Thus, the reductive pretreatments result in more stable catalysts (lower deactivation), while the activity is highest for the calcined catalysts, both the initial and the steady-state activity. The decreasing difference between the activities of differently

pretreated catalysts indicates that with ongoing reaction the pretreatment induced differences in surface composition become less important and the catalyst surfaces more and more resemble each other.

Comparison of the activities and the deactivation at 300 °C reaction temperature with previously reported results obtained under similar reaction conditions is not possible, since most studies of the water gas shift reaction were performed at lower temperatures and/or in different reaction gas mixtures (for an overview see ref. [14]). Focusing on Au/CeO_2 catalysts and high reaction temperatures, the following studies are relevant: Fu et al. [31] determined a comparable rate of 4.2×10^{-3} mol g_{Au}^{-1} s^{-1} at 300 °C, but in a different, more realistic gas mixture (11% CO, 7% CO_2, 26% H_2O, 26% H_2, 4.7 wt.% Au/CeO_2, calcination at 400 °C). Under these reaction conditions, they observed an almost constant activity over 120 h of reaction [31,32]. Similar findings were reported by Andreeva et al., who found their Au/CeO_2 catalysts to be very stable during the WGS reaction over a wide temperature range (reaction temperature 140–50 °C, 1–5 wt.% Au/CeO_2, 1 h reduction in 1% H_2/Ar at 100 °C, gas mixture 5% CO, 30% H_2O and Argon) [33]. They proposed that the deactivation (by Au nanoparticle sintering) is counteracted by a re-dispersion of the Au particles (decreasing particle size) during the reaction. On the other hand, there are a number of studies reporting a pronounced deactivation of Au/CeO_2 or related catalysts during the WGS reaction under comparable reaction conditions. Luengnaruemitchai et al. observed a strong deactivation (83%) after 48 h WGS reaction at 360 °C in 2% CO and 20% H_2O on a 1 wt.% Au/CeO_2 catalyst (calcination at 500 °C in air for 5 h), while on Pt/CeO_2 no significant deactivation was detected [34]. Despite of the drastic pretreatment conditions, the Au particles grew from 4 to 5.5 nm during the reaction, which was considered as being responsible for the deactivation [34]. A fast and considerable loss of activity (about 50%) was reported also for reaction on a Au/CeO_2 catalyst at 240 °C (10% CO, 22% H_2O, 6% CO_2, 43% H_2 and 19% N_2, 5 wt.% Au/CeO_2, reduction in a mixture of 4% H_2/N_2 for 4 h) by Kim and Thompson [22]. These authors, however, attributed the deactivation to an increasing surface blocking by adsorbed carbonate and/or formate species, which are produced during WGS reaction. This assignment is close to the current understanding of the deactivation at lower reaction temperatures, which is due to accumulation of stable monodentate surface carbonate species [14–16]. A very different mechanism for deactivation was put forward by Zalc et al. for the WGS reaction on a Pt/CeO_2 catalyst (pre-calcined at 500 °C, reaction at 250 °C) [35]. They proposed that an irreversible (over)reduction of the ceria support in the H_2-rich feed gases is responsible for the deactivation. As mentioned before, a consistent explanation of the different results is hardly possible because of the pronounced differences in the reaction conditions between these measurements. Au nanoparticle sintering, however, appears to be questionable as dominant factor at reaction temperatures around 300 °C.

In our previous measurements on a 2.7 wt.% Au/CeO_2 at 180 °C in 1% CO, 2% H_2O, N_2 for H400 and O400 pretreated samples [16], we also obtained a higher activity on the O400 sample, while the deactivation in those measurements was more pronounced on the H400 sample. This may indicate a different reaction mechanism at
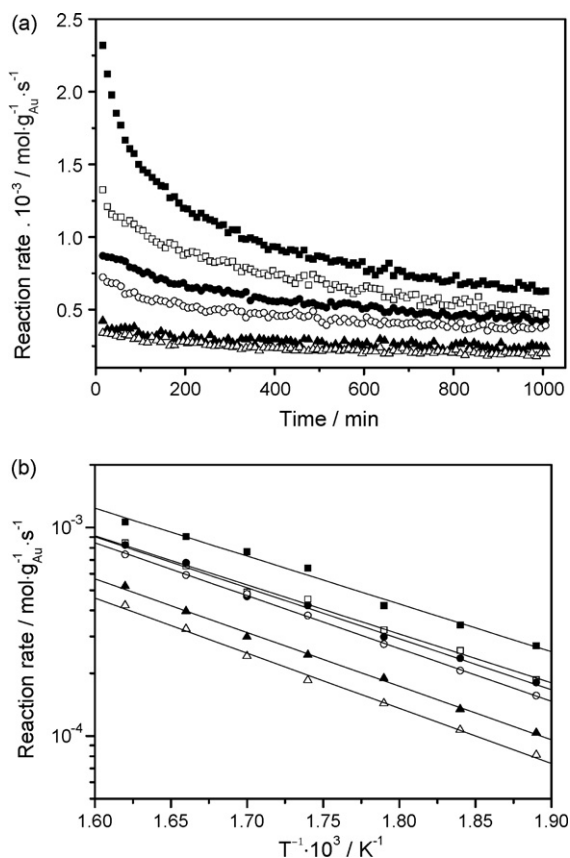

Fig. 1. (a) Temporal evolution of the activity (deactivation) on differently pretreated Au/CeO_2 catalysts in the WGS reaction in idealized reformate (1% CO, 2% H_2O, rest N_2) at 300 °C. (b) Arrhenius plot of the temperature dependent reaction rates on the differently pretreated catalysts after 1000 min WGS reaction and subsequent measurements at the various temperatures (1 h each). Pretreatment: (■) O400, (□) H400/O400, (●) N400, (○) CO400, (▲) O400/H400 and (△) H400 (parameters see Section 2.1).

low temperature (180 °C) than at higher temperatures (300 °C). A similar suggestion of a change in dominant reaction pathway upon going to higher temperatures was made earlier already by Tibiletti et al. [14,36]. They had proposed that the dominant reaction pathway for the WGS reaction on Au/CeO$_2$ catalysts (and previously also for other catalysts such as Pt/ZrO$_2$ [36]) will change with temperature, with the dominant reaction pathway at lower temperatures involving formation and decomposition of formate, carbonate or carboxylate species, while for higher temperatures, a redox mechanism involving reduction and reoxidation of ceria was proposed to be dominant [14].

For further information on a possible change in the dominant reaction pathway with temperature, we determined the apparent activation energies from activity measurements in the temperature range of 250–350 °C (1 h at each temperature), after an initial deactivation run of 1000 min. The temperature dependent rates after different pretreatments are shown in the Arrhenius plot in Fig. 1b, the resulting apparent activation energies are listed in Table 1. Most of the values are around 45 ± 2 kJ mol^{-1}, only for reductive pretreatment somewhat higher values are obtained (51 ± 1 kJ mol^{-1}). For reaction at 180 °C under similar reaction conditions, we recently determined activation energies of 40 ± 2 kJ mol^{-1} on 1.4–12.6 wt.% Au/CeO$_2$ catalysts (pretreatment at 200 °C in H$_2$ (H200), measurements in the temperature range between 80 and 180 °C in idealized reformate (1% CO, 2% H$_2$O, N$_2$) [21]. The differences in the apparent activation energies at lower and higher temperatures are small, but outside the uncertainty of the measurements. Hence, these data do not provide clear evidence for a change in mechanism between 180 and 300 °C, but it cannot be ruled out either.

3.2. Catalyst surface properties before and after WGS reaction

The chemical composition of the catalyst after different pretreatments and after additional 1000 min WGS reaction was characterized via the Au(4f) and Ce(3d) signals. The main XPS results are listed in Table 2, Au(4f) spectra are plotted in Fig. 2. For quantitative evaluation, the XP spectra of the Au(4f) signals were fitted by three different states, with BEs of 84.0, 84.6 and 85.9 eV, respectively [8,31,37,38]. The first and the last peaks are assigned to Au^0 and Au^{3+} species [27,37,39]. A peak at 84.6 eV was previously attributed to Au^{1+} species [8,31]. As discussed in detail elsewhere [18,40], we explain the intensity at BEs slightly above the Au^0 peak by very small neutral Au particles, whose BE is upshifted due to particle size effects ('final state effects') [41–43]. For a realistic particle size distribution, this would create a sequence of Au(4f) states, with the BE varying with Au particle size. For practical purposes (and because of the unknown distribution of BEs), the resulting intensity distribution is described by a single peak of adjusted peak width (Au$^{0'}$ peak). One should keep in mind, however, that because of the variations in particle size distributions after different pretreatments or after reaction this can only be an
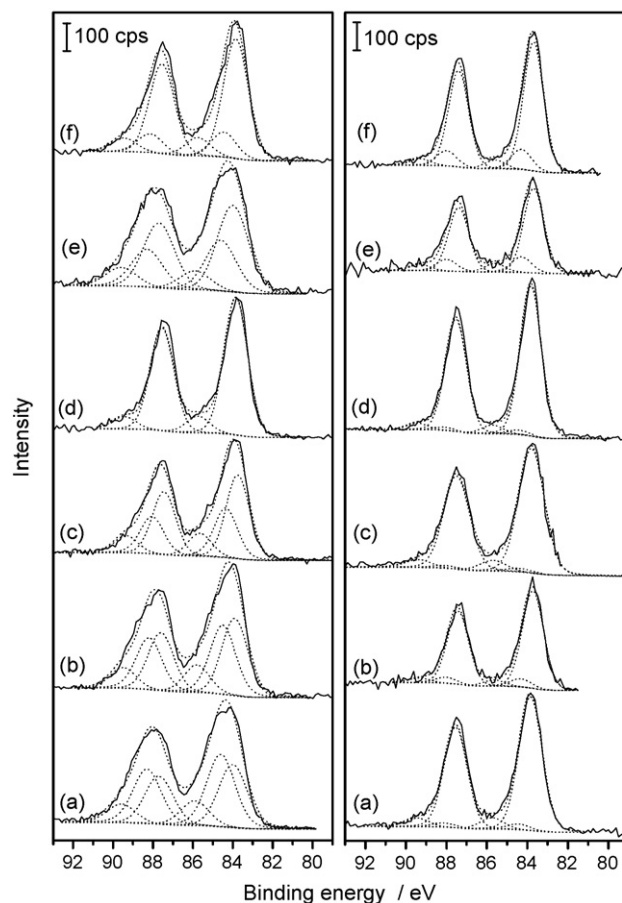

Fig. 2. XP spectra of the Au(4f) region of a 4.5 wt.% Au/CeO$_2$ catalyst recorded after pretreatment (left panel) and after 1000 min WGS reaction in idealized reformate at 300 °C (right panel). Pretreatment: (a) O400, (b) H400/O400, (c) N400, (d) CO400 (e) O400/H400 and (f) H400 (parameters see Section 2.1).

approximate description of the contribution from very small Au nanoparticles.

After oxidative pretreatment (O400), the XP spectra (Fig. 2, left panel) show the highest amount of Au^{3+}, it decreases in the order O400 > H400/O400 > N400 > O400/H400 > H400 > CO400. Also the Au$^{0'}$ contribution follows this order. As expected, the reductive pretreatment leads to stronger reduction and Au^0 formation than purely thermal treatment or even oxidative treatment. Accordingly, the Au^0 content decreases in the order CO400 > H400 > O400/H400 > N400 > H400/O400 > O400. For Ce^{3+}, the differences are much smaller, but follow the same tendency as observed for Au^0.

Table 2
Catalyst properties of a 4.5 wt.% Au/CeO$_2$ catalyst after different pretreatment procedures, after 1000 min WGS reaction, and before/after reaction of a O400 (H400) pretreated catalyst by an O400 (H400) reactivation procedure

Catalyst treatment	Au^0 (%)		Au$^{0'}$ (%)		Au^{3+} (%)		Ce^{3+} (%)		$I_{Au(4f)}/I_{Ce(3d)}$		XRD Au(1 1 1) (nm)	
	Before	After	Before	After	Before	After	Before	After	Before	After	Before	After
O400	35	88	45	4	20	8	21	23	0.08	0.06	2.9 ± 1.0	3.6 ± 1.0
H400/O400	43	87	41	8	16	6	25	25	0.08	0.04	NM	NM
N400	53	89	33	3	15	8	23	26	0.06	0.06	NM	NM
CO 400	89	92	0	3	11	6	25	27	0.06	0.06	NM	NM
O400/H400	54	78	33	14	13	8	23	25	0.08	0.04	NM	NM
H400	73	81	16	14	11	6	24	25	0.07	0.06	2.6 ± 1.0	3.2 ± 1.0
O400 reactivation	88	67	4	17	8	16	23	24	0.06	0.06	NM	NM
H400 reactivation	81	79	14	13	6	8	25	25	0.06	0.05	NM	NM

The ratio of the Au and Ce related intensities, the $I_{Au(4f)}/I_{Ce(3d)}$ ratio, contains information on the Au particle size. The resulting values and, where available, also the results from XRD measurements, are listed in Table 2. After pretreatment in O_2 (O400) or H_2 (H400), we obtain almost similar values of 0.08 or 0.07 ± 0.01 for this ratio, indicating similar Au particle sizes after the two procedures. This qualitative conclusion is confirmed by XRD measurements, which show comparable Au particle sizes after O400 (2.9 ± 1.0 nm) and H400 (2.6 ± 1.0 nm) pretreatment. The values after N400 and CO400 pretreatment (0.06 ± 0.01) are slightly lower, but the difference to the other values is still within the experimental limit. Hence, based on the present data, we have no indication for significant differences in the Au particle sizes after the different pretreatment procedures. In earlier XPS and XRD measurements on comparable 2.7 wt.% Au/CeO$_2$ catalysts after reductive and oxidative pretreatment, we found that for 200 °C pretreatment the reductive processing leads to larger particles sizes compared to oxidative pretreatment, while for pretreatment at 400 °C the particle sizes were rather similar [16].

The influence of the different pretreatments on the nature and abundance of adsorbed species was investigated by *in situ* DRIFTS measurements. Spectra recorded in N_2 at 300 °C directly after catalyst conditioning are shown in Fig. 3. (Note that the spectra are rescaled to similar background intensity to remove effects due to changes in the reflectivity.) Most obvious are the differences in the OH stretch and in the OCO bending vibration regions. In the OH region, all spectra exhibit three peaks at 3520, 3735 and 3631 cm^{-1}, which were assigned to monodentate and tridentate OH$_{ad}$ groups on ceria [44]. After reductive pretreatments, an additional peak at 3649 cm^{-1} appears. This signal was previously attributed to bridged OH$_{ad}$ groups [45,46]. Since it was also observed after CO400 treatment, where additional hydrogen uptake is impossible, OH$_{ad}$ species with similar vibrational properties can be generated also by modification of existing OH$_{ad}$ species due to ceria surface reduction. From the present data we cannot decide, however, whether the formation of these OH$_{ad}$ species is strictly related to the reduction of the surface or whether it can be generated also on non-reduced surface areas under reaction conditions if hydrogen or water are present. (Note that the signals in the C–H region (2700–3000 cm^{-1}), normally indicative of adsorbed formates, are caused by contaminants on the IR mirrors.)

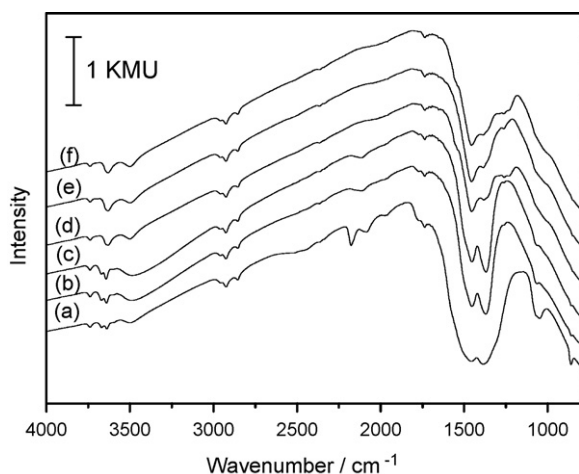Independent of the pretreatment, bands in the range between 1250 and 1550 cm^{-1} show characteristic features for carbonate species (Fig. 3), which due to the absence of CO or CO$_2$ in the pretreatment atmosphere must be present on the catalyst already prior to conditioning [47]. Complete removal of these carbonate species from ceria surfaces by thermal decomposition was reported to require temperatures up to 1000 °C [48], which in the presence of Au may be somewhat lower [17,49]. On all samples, we find a dominant peak at ~1454 cm^{-1}, which was assigned previously to a not further specified 'bulk carbonate' [50,51]. An additional peak, which appears at ~1368 cm^{-1} after reductive conditioning and at ~1385 cm^{-1} after oxidative pretreatment or drying in N_2, was assigned to monodentate carbonate species [45]. Finally, a weak feature is resolved at ~1550 cm^{-1} in the intensity decay below 1600 cm^{-1}, which was attributed to an unspecified carbonate species [52]. A feature in this frequency is likely to exist also on the reductively pretreated catalysts, but it cannot be resolved from the decaying background. Comparable spectra were observed also by Karpenko et al. [16].

In the CO$_{ad}$ region, a peak at 2118 cm^{-1} obtained after reductive treatments (H400, O400/H400 and CO400) is related to an electronic excitation from donor levels located near the conduction band such as Ce^{3+} or oxygen vacancies [50,53,54]. Two additional bands at 2080 and 2176 cm^{-1}, which appear after conditioning in CO atmosphere at 400 °C, are related to CO adsorbed on negatively charged Au$^{\delta-}$ species [20,55] and on Ce^{4+} ions [52,56–58]. The Au$^{\delta-}$ species are created by an electron transfer from oxygen vacancies on the partly reduced support surface to the Au particles [20,55].

In total, the data are in good agreement with previous measurements in our group on a 2.7 wt.% Au/CeO$_2$ catalyst [16]. As expected, most H_2O is present after H_2 reductive pretreatment; most likely this is true also for OH$_{ad}$ species, although these intensities are hard to quantify because of the overlap with the water signal at ~3300–3500 cm^{-1}. On the other hand, the content of surface carbonates is highest after CO400 pretreatment. The carbonate positions differ for the reductive and oxidative pretreatment or drying at 400 °C, and oxidative pretreatment increases the carbonate decomposition. This latter result agrees well with the observed higher initial activity of oxidatively pretreated catalysts (less surface carbonates).

Reaction induced changes in surface composition

The differences in surface composition observed after the different pretreatment procedures are still present also after 1000 min reaction, but they are much less pronounced. This confirms our previous tentative conclusion, that with ongoing exposure to the reaction atmosphere, the pretreatment related differences in catalyst surface composition disappear increasingly. The catalysts more and more resemble each other, as it was indicated already by the decreasing differences between initial and steady-state activity (see above). The contributions from the different Au species and from Ce^{3+} are listed in Table 2, Au(4f) detail spectra are plotted in Fig. 2 (right panel). In all cases, the reaction atmosphere and the high reaction temperature have a reducing effect on the Au/CeO$_2$ catalyst. This is reflected by a pronounced increase of the Au^0 contribution, except for the H400 and, even more clearly, for the CO400 sample, where this component was dominant already after pretreatment. Interestingly, the two H_2 treated samples, H400 and O400/H400, have a markedly higher Au$^{0'}$ contribution after reaction than all other samples, while the Au^{3+} content after reaction is about similar for all catalysts. The Ce^{3+} content increased slightly for all catalysts, independent of pretreatment. Because of their small extent, on the order of 1–2%, the changes would be negligible, if they were not positive for all samples.

During the WGS reaction, the $I_{Au(4f)}/I_{Ce(3d)}$ ratio decreased slightly, with the reaction induced change in intensity ratio

Fig. 3. DRIFT spectra (raw data, normalized to the same reflectivity) of the Au/CeO$_2$ catalysts recorded in N_2 at 300 °C after different pretreatments: (a) CO400, (b) H400, (c) O400/H400, (d) N400 (e) H400/O400 and (f) O400 (parameters see Section 2.1).

decreasing in the order O400 = H400 > H400/O400 = O400/H400 > O400 > H400 > N400 = CO400 = 0. Also in this case, the changes are often within the limits of resolution. Since in all cases the reaction results in a decrease of this value, we consider these changes nevertheless to be significant. They point to a slight reaction induced decrease of the Au dispersion, equivalent to a similarly small increase of the mean Au particle size. This is confirmed by XRD measurements for the O400 and H400 samples, which yield an increase of the mean Au particle size from 2.9 to 3.6 nm (O400) and from 2.6 to 3.2 nm (H400) (in all cases ± 1 nm). The small, but not negligible increase in Au particle size during 1000 min of reaction differs from our findings for reaction at 180 °C, where changes in particle size were essentially absent [19]. On a quantitative scale, however, the changes in Au dispersion during the reaction are too low to contribute significantly to the observed rapid deactivation of the catalysts during reaction.

3.3. Accumulation of adsorbed reaction intermediates during the WGS reaction

The accumulation of adsorbed reaction intermediates and side products during the WGS reaction on the differently conditioned catalysts, under similar conditions as applied for the activity measurements (1% CO, 2% H_2O, rest N_2, at 300 °C), was followed by *in situ* IR spectroscopy (DRIFTS) measurements. Sequences of spectra recorded during reaction are presented in Fig. 4a–f. Each set of spectra shows the entire spectrum (bottom) as well as details of the CO_{ad}/CO_2 region (middle left), of the OCO region (middle right), of the O–H region (top left) and of the C–H region (top right). Independent of the pretreatment, the same characteristic features develop during reaction. For a quantitative evaluation of the reaction induced modifications in the adlayer, we plotted in Fig. 5 the integrated peak intensities/heights of the CO_2 peak at 2363/2331 cm^{-1} (peak intensity), the bidentate formate peak at 2828–2833 cm^{-1} (peak height) and of several peaks in the OCO bending region (peak heights) as a function of time. The latter group included the bidentate carbonate related peak at 1281–1310 cm^{-1}, a monodentate carbonate related peak at 1397–1405 cm^{-1} (reductive pretreatment)/1368–1372 cm^{-1} (oxidative or N_2 pretreatment), the carbonate related peak at 1520–1522 (oxidative or N_2 pretreatment)/1540 cm^{-1} (reductive pretreatment) and finally the formate related peak at 1582–1590 cm^{-1} [52]. Also these data were corrected for reaction induced changes in the reflectivity.

OH region

The different peaks in this range (3588, 3630, 3670 and 3649 cm^{-1}) were assigned already in the last section (see also ref. [21]). On the reductively pretreated catalysts, no new peaks appear during the reaction, only the intensities of the different OH_{ad} species change slightly with time. On the oxidatively pretreated or dried samples, the peak at 3649 cm^{-1}, which was not present after pretreatment, develops at the beginning of the reaction. This peak was assigned to a bridged OH_{ad} group, which is considered as educt for formate formation [21,46,59]. Its intensity decreases slightly during the reaction, with little difference between the different pretreatments.

CH region

The peaks in this range are related to C–H vibrations of different surface formate species, including bidentate formates (2828–2833 cm^{-1}) and bridged formate (2941 cm^{-1}) as well as a controversially assigned formate species with a signal (shoulder) at 2875 cm^{-1} [47]. These C–H signals are accompanied by OCO bending vibrations at ∼1590 cm^{-1} (antisymmetric) and 1373 (symmetric) on the differently pretreated catalysts [45,47]. During the reaction, the intensity of the bidentate formates increases in the beginning of the reaction and starts to decrease after 1–10 min reaction, independent of the pretreatment. Higher intensities were observed after reductive pretreatment, lower ones after pretreatment in oxidative or inert atmosphere, indicating a faster formate decomposition in the latter cases.

OCO bending region

The signals in the OCO region (1200–1600 cm^{-1}), which vary for the different pretreatments (see last section), overlap considerably. On the reductively pretreated catalysts, peaks related to carbonates appear at 1540 (carbonate), 1397–1405 (monodentate carbonate) and 1291 cm^{-1} (bidentate carbonate). The first two peaks grow rapidly in intensity at the beginning of the reaction, until after 30 min the further increase is significantly slower. The bidentate carbonate signal also increases rapidly in intensity, but passes through a maximum after 30 min and then decreases again. (Note that the peak at 1397–1405 cm^{-1} existed already before reaction; see Fig. 3.) It is not visible in the first spectrum since it is comparable to the background spectrum which was subtracted from the reaction spectra.) For the catalyst pretreated in oxidative or inert atmosphere, the peak positions are slightly different (carbonate at 1522 cm^{-1}, monodentate carbonate at 1368 cm^{-1}, bidentate carbonate 1302–1310 cm^{-1}). The behavior of the carbonate and bidentate carbonate intensity with time resembles that on the reductively pretreated catalyst, while for the monodentate carbonate signal the intensity is significantly higher than on the latter catalysts. The peak at 1454 cm^{-1}, which is dominant before reaction on all catalysts (see Fig. 3), does not seem to change in intensity during the reaction. At least, this cannot be resolved from the strong increase of the carbonate signals at 1368–1405 cm^{-1} and 1522–1540 cm^{-1}, respectively.

CO_{ad}/CO_2 region

In the CO_{ad} region (2000–2200 cm^{-1}), a peak at 2117 cm^{-1} appears after oxidative pretreatment, which is usually related to CO adsorbed on Au [60–62]. Alternatively, this peak could also be related to an electronic transition from donor levels located near the conduction band such as Ce^{3+} or oxygen vacancies [53], as it was observed after reductive pretreatment (Fig. 3). In view of the H_2O content in the reaction atmosphere, however, this is unlikely. The signals initially increase in intensity for the first 5 min, and then remain about constant. Because of the high temperature, the steady-state coverage and hence also the IR intensity are very low throughout the reaction. On the reductively pretreated catalysts, the CO_{ad} signal was almost absent. This can be explained by two counteracting effects, the removal of the peak visible in the spectra in Fig. 3, which was related to an electronic transition as described above, in the reaction atmosphere, and the build-up of the CO_{ad} related peak. Looking at the intensities in Fig. 3 and in the CO_{ad} peaks on oxidatively pretreated catalysts, these contributions should almost cancel out, which is indeed the case. After CO400 conditioning, negative peaks at 2072 and 2178 cm^{-1} reflect the partial removal of adsorbed CO during the WGS reaction (see also Section 3.2).

The CO_2 related intensity, which is coupled with the CO_2 formation and hence the activity of the catalyst, follows similar trends as the activities determined in the kinetic measurements (Fig. 1). It is highest after O400 pretreatment, and decreases in the same order: O400 > H400/O400 > N400 > CO400 > O400/H400 > H400 (Fig. 4). The relative decay of the CO_2 intensity after 1000 min reaction, by
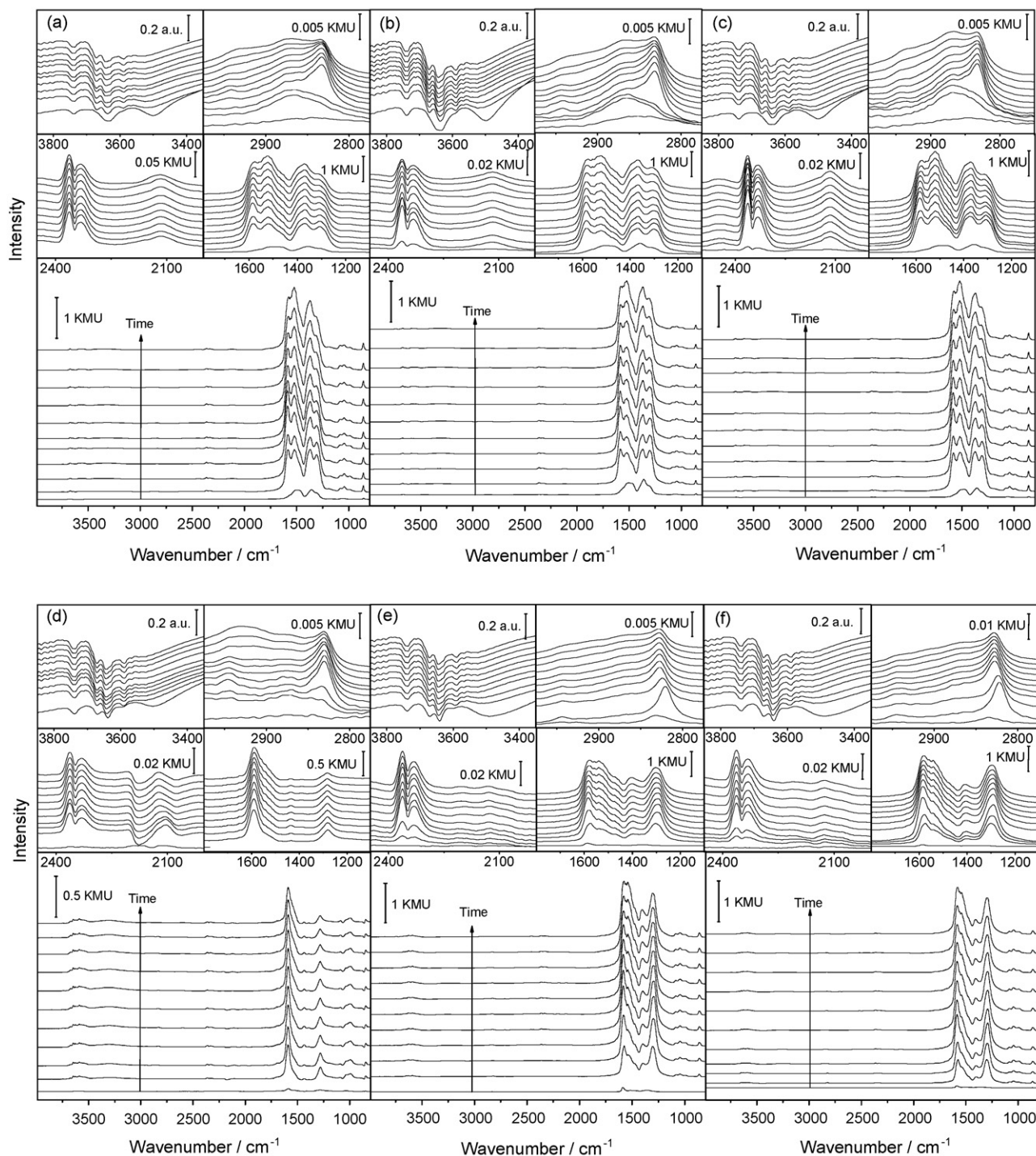
Fig. 4. Sequence of DRIFT spectra recorded during 1000 min WGS reaction in idealized reformate at 300 °C on a 4.5 wt.% Au/CeO$_2$ catalyst after different pretreatments: (a) O400, (b) H400/O400, (c) N400, (d) CO400 (e) O400/H400 and (f) H400 (parameters see Section 2.1). The IR-regions are displayed in the following order from bottom to top: full spectrum (bottom), OCO region (middle left), CO$_{ad}$/CO$_2$ region (middle right), C–H region (top left) and O–H region (top right). The spectra displayed are recorded after 24 s, 48 s, 1 min, 5 min, 10 min, 30 min, 60 min, 120 min, 360 min, 600 min and 1020 min.

33% and by 15% after O400 and H400, respectively, is lower than the observed deactivation in Fig. 1a (deactivation by 73% after O400 and by 43% after H400), but the trends are comparable. The quantitative differences are presumably related to the fact that in the DRIFTS measurements the conversions are higher [40].

Comparing our results with the reaction at 180 °C shows that the relative temporal evolution of the OH, formate, carbonate and CO$_2$ intensity is similar in both cases. The absolute intensities

of the CO$_2$ signal are even higher compared to the reaction at 180 °C [15,16], while the formate intensity is lower, which fits well to the higher activity at 300 °C. The absolute carbonate intensity is higher after reaction at 300 °C than after 180 °C reaction [15,16]. The decrease of the bidentate formate intensity after passing through an initial maximum, independent of the pretreatment, as well as its correlation with the activity for CO$_2$ formation – the highest intensity was observed after reductive pretreatment
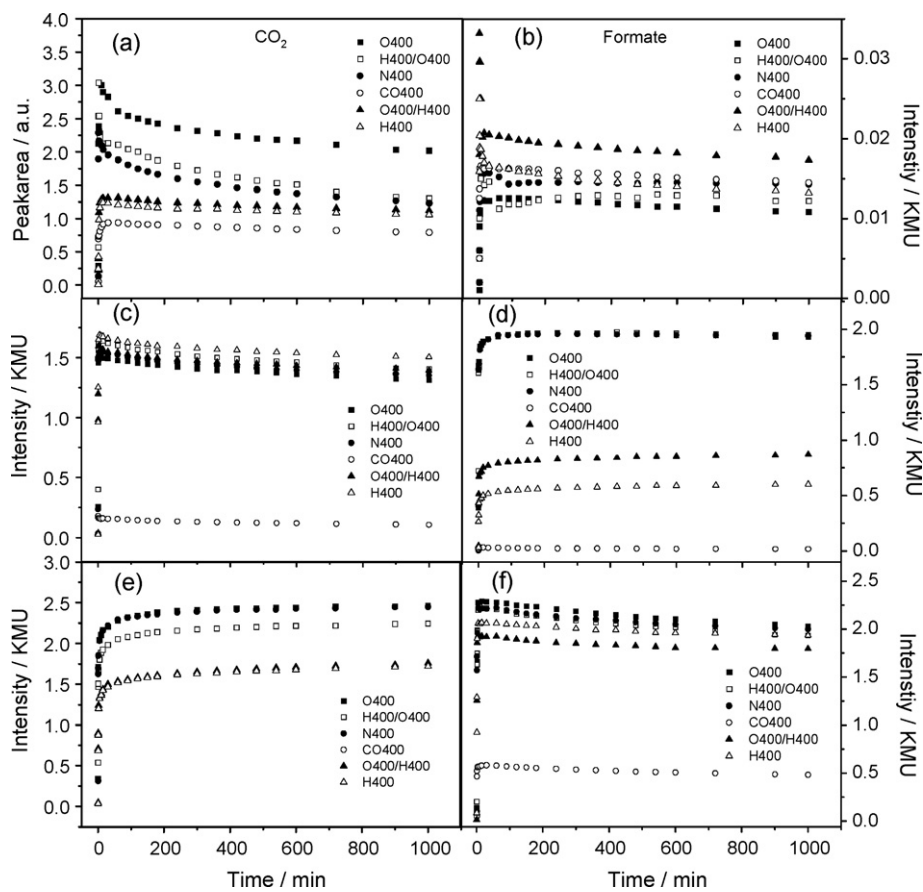
Fig. 5. Time evolution of the integrated intensities (after normalization to different reflectivities and background subtraction) of different peaks in the DRIFT spectra in Fig. 4 during WGS reaction in idealized reformate on differently pretreated 4.5 wt.% Au/CeO_2 catalysts at 300 °C. (a) CO_2 intensity (2332/2363 cm^{-1}), (b) bidentate formate intensity (2832 cm^{-1}), (c) bidentate carbonate intensity (1281–1310 cm^{-1}, peak height), (d) monodentate carbonate intensity (1397–1405 cm^{-1} after reductive pretreatment/1368–1372 cm^{-1} after oxidative and N_2 pretreatment, peak height), (e) carbonate peak (1520–1522 cm^{-1} after oxidative and N_2 pretreatment/1540 cm^{-1} after reductive pretreatment); (f) formate related intensity (1582–1590 cm^{-1}, peak height). The respective pretreatments are given in the figure.

and the lowest after pretreatment in oxidative or inert atmosphere – indicate a close connection between bidentate formate formation/decomposition and CO_2 formation in the latter cases. This agrees well with our earlier proposal of bidentate formate species acting as reaction intermediates in the dominant reaction pathway and their decomposition as rate limiting step for the WGS reaction at 180 °C [21]. Furthermore, the intensities of bidentate carbonates decrease, while those of the other stable carbonates, which were associated with the catalyst deactivation [15,16], increase with time for all catalysts. These trends further support our earlier conclusions that the general characteristics of the WGS reaction on Au/CeO_2 catalysts do not change between 180 and 300 °C.

Comparing the IR data and the activity measurements on the one hand with the variation of the chemical state of Au on the differently conditioned catalysts on the other hand shows no clear correlation. The highest initial activity was observed with the highest amount of Au^{3+} and $Au^{0'}$. Fu et al. [8,31] proposed that the activity correlate with Au^{1+} species, while Au^0 act only as spectator. Note that this Au^{1+} peak at about 0.6 eV up-shifted BE compared to metallic Au, is identical to the $Au^{0'}$ peak. Based on measurements on Au leached Au/CeO_2 catalysts, Karpenko et al. proposed that the Au^{3+} species and the small $Au^{0'}$ Au particles are highly active for formate formation, while the Au^0 particles were more active for formate decomposition [18]. Following that scheme, we would expect a lower formate formation rate and a higher formate decomposition rate and hence a lower formate coverage after reductive treatment compared to an oxidatively pretreated catalyst, which is opposite

to our findings. With ongoing WGS reaction, the difference in abundance of the different Au states between the differently pretreated catalysts decreases, after 1000 min mainly metallic Au^0 (78–92%) is present. Accordingly, the rate for formate decomposition should go up, resulting in a lower steady state formate coverage, in agreement with observations.

Finally, the close correlation between catalyst deactivation, decreasing CO_2 related IR signal and increasing monodentate carbonate related IR intensity, which is independent of the catalyst pretreatment, indicates that the deactivation is related to and presumably caused by the build-up of stable (monodentate) surface carbonate species with time. This agrees fully with previous results for reaction at 180 °C, where monodentate surface carbonates were identified as main cause of catalyst deactivation [15,19,22,23]. The build-up of stable surface carbonates can (i) block active sites for reaction intermediate (formate) formation and/or decomposition and/or (ii) block the access of adsorbed reaction intermediates (formates) to the active sites [15,17].

3.4. Reactivation of the Au/CeO_2 catalyst

Further information on the physical origin of the catalyst deactivation in the WGS reaction can be obtained from reactivation experiments [19,23,24]. If the formation of adsorbed carbonate species on the catalyst were the main reason for the deactivation during the WGS reaction, as it was proposed in several studies [15,19,22,23], it should be possible to at least partly recover the

initial activity by thermal/thermochemical decomposition of the carbonate. This can be done, e.g., by reaction with O_2 or water at elevated temperatures [15,19,22,24], or by heating in N_2 up to 500 °C [23]. In this section, we study the effect of reactivating the Au/CeO$_2$ catalysts after 1000 min reaction, employing the pretreatment process also for reactivation. Since the differences in the chemical composition, activity/stability and formation of adsorbed surface species were largest between oxidative (O400) and reductive (H400) pretreatment, respectively, we used these procedures for pretreatment and for reactivation.

Fig. 6 shows the evolution of the WGS reaction rates on both catalysts before and after reactivation. For better comparison, the curves were normalized to the respective initial activities (r_0) after 16 min reaction. The initial activity of the O400 pretreated catalyst could be restored almost completely (95%) by re-oxidation for 30 min in 10% O_2/N_2 at 400 °C. After reactivation, the reaction rate decayed with time in the same way as it was observed for the freshly prepared catalyst in the initial phase of the WGS reaction. For H400 reactivation (30 min in 10% H_2/N_2 at 400 °C) of a H400 pretreated catalyst, the results are markedly different. Reactivation effects are hardly visible. After reactivation, the activity was close to that measured after 1000 min WGS reaction, and also the further decay followed closely that extrapolated from the first 1000 min reaction for longer times. This result of a drastic reactivation effect upon annealing in O_2 containing atmosphere (O400 pretreated catalyst) and little effect for reductive treatment (H400 pretreated catalyst) agrees closely with our results obtained for reactivation of Au/CeO$_2$ catalysts deactivated during reaction at 180 °C [19], which also points to a similar physical origin for deactivation at the two reaction temperatures.

The results of XPS measurements performed directly after reconditioning are summarized in Table 2. Within the precision of the measurements, the intensity of the Ce^{3+} species remained constant for both the H400 and the O400 reactivated catalyst. This underlines that the slight increase of the Ce^{3+} intensity during the WGS reaction is not a major cause for the deactivation, in contrast to a deactivation mechanism based on the overreduction of the support, which was proposed for the deactivation of Pd/CeO$_2$ catalysts during the WGS reaction [35]. For Au species, the effect of reactivation is more pronounced, at least for O400 reactivation. In that case, the Au^0 content decreases from 88% (after 1000 min reaction) to 67% (after reactivation), while the Au$^{0'}$ and Au^{3+} contents increase accordingly, from 4 to 17% (Au$^{0'}$) and from 8 to 16% (Au^{3+}). Hence,

a fraction of the Au nanoparticles are dispersed under reactivation conditions to substitutional Au^{3+} [63] and small Au clusters (see above). On the other hand, for H400 reactivation, the changes in the distribution of Au species are rather small. Finally, the $I_{Au(4f)}/I_{Ce(3d)}$ ratio is comparable to that before reactivation, with values of 0.06 and 0.05 after O400 and H400 reactivation, respectively. This latter result provides further evidence for our conclusions that also for reaction at 300 °C Au particle sintering plays only a minor role for the deactivation of Au/CeO$_2$ catalysts.

To further investigate the effect of catalyst regeneration on the adsorbed species present on the catalyst surface after 1000 min WGS reaction, we performed DRIFTS measurements during the reaction, before and after the O400 and H400 reactivation, respectively. (Note that during reactivation at 400 °C the intensity of the spectra is too low for meaningful measurements because of the reduced reflectivity.) Time sequences of selected spectra are shown in Fig. 7, with O400 reactivation in the left panels and H400 reactivation in the right panels. From top to bottom, the panels show details of the OCO region, of the CO$_{ad}$/CO$_2$ region and of the CH region. The effect of the reactivation procedure is visible by comparing the first spectrum (last spectrum before reactivation) and the second spectrum (first spectrum after reactivation, started before the reaction atmosphere has reached the DRIFTS cell (0 s)). This comparison shows that independent of the reactivation procedure, all formate species and of course also the CO$_{ad}$ and CO$_2$ species disappeared upon reactivation. For surface carbonate species (OCO region), the situation is different. These are completely removed after O400 reactivation, with the intensity decreasing to the initial intensity on a freshly conditioned catalyst. For H400 reactivation, the formate ($\sim$1580 cm^{-1}) and bidentate carbonate (1294 cm^{-1}) related peaks disappear or decrease in intensity, while the monodentate carbonate related intensity at $\sim$1405 cm^{-1} decreased by 60%. It should be noted that the carbonate coverage and the WGS activity are not necessarily linearly coupled. Even for a significant reduction in carbonate coverage the reaction inhibiting blocking of active sites may be maintained. In total, H400 treatment is much less efficient for carbonate decomposition than annealing in O_2. Oxygen assisted carbonate decomposition was found to be active on Au/CeO$_2$ already at 120 °C in recent TAP reactor (temporal analysis of products) measurements [64]. This result in combination with the results of the kinetic measurements discussed above fully agrees with our interpretation that stable surface carbonates are the main reason for Au/CeO$_2$ catalyst deactivation during the WGS reaction also at 300 °C reaction temperature. Furthermore, the data indicate that the bidentate carbonates have little effect on the WGS activity of the catalyst.

During the WGS reaction following the reactivation procedure, the same surface species appeared as observed during the initial phase of the reaction on the freshly prepared catalyst (for O400 reactivation) or before the reactivation procedure (for H400 reactivation). After reaching steady-state conditions for the reversible adsorbates (CO$_{ad}$, formate, bidentate carbonates (1294 cm^{-1})), their intensities as well as the CO$_2$, intensity decrease again, while that of other carbonates increases with time for all catalysts. Thus, deactivation occurs again after passing the gas mixture due to the build-up of carbonate species with time.

Liu et al. [23] and Hilaire et al. [24] reported similar results. They showed that catalyst regeneration by calcination in air at 400 and 500 °C completely removes the carbonates formed on the catalysts (Pt/CeO$_2$, Pd/CeO$_2$) during the WGS reaction. Au/CeO$_2$ catalysts were reported to regain more than 95% of their initial activity for the WGS reaction at 240 °C after using the same procedure for reactivation as initially used for conditioning of the fresh catalyst (calcination in air at 400 °C with following reduction in a mixture of 5% H_2/N_2) [22]. This deactivation was related to the
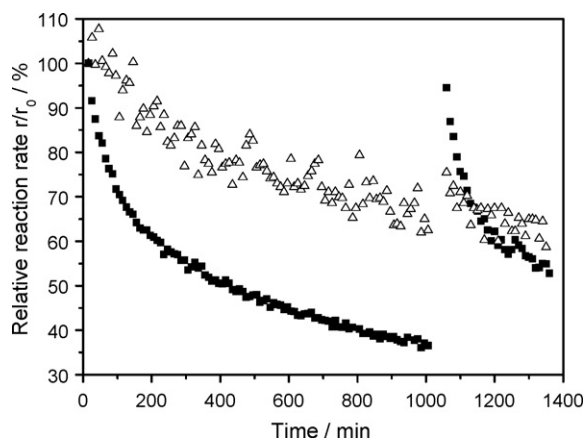

Fig. 6. Relative reaction rate (r/r_0), where r_0 denotes the initial reaction rate recorded after 16 min WGS reaction, on a 4.5 wt.% Au/CeO$_2$ catalyst at 300 °C in idealized reformate after reductive ($\triangle$, H400) and oxidative ($\blacksquare$, O400) pretreatment over 1000 min reaction time, subsequent reactivation applying the same procedure as used for conditioning before, and further WGS reaction up to 1400 min.
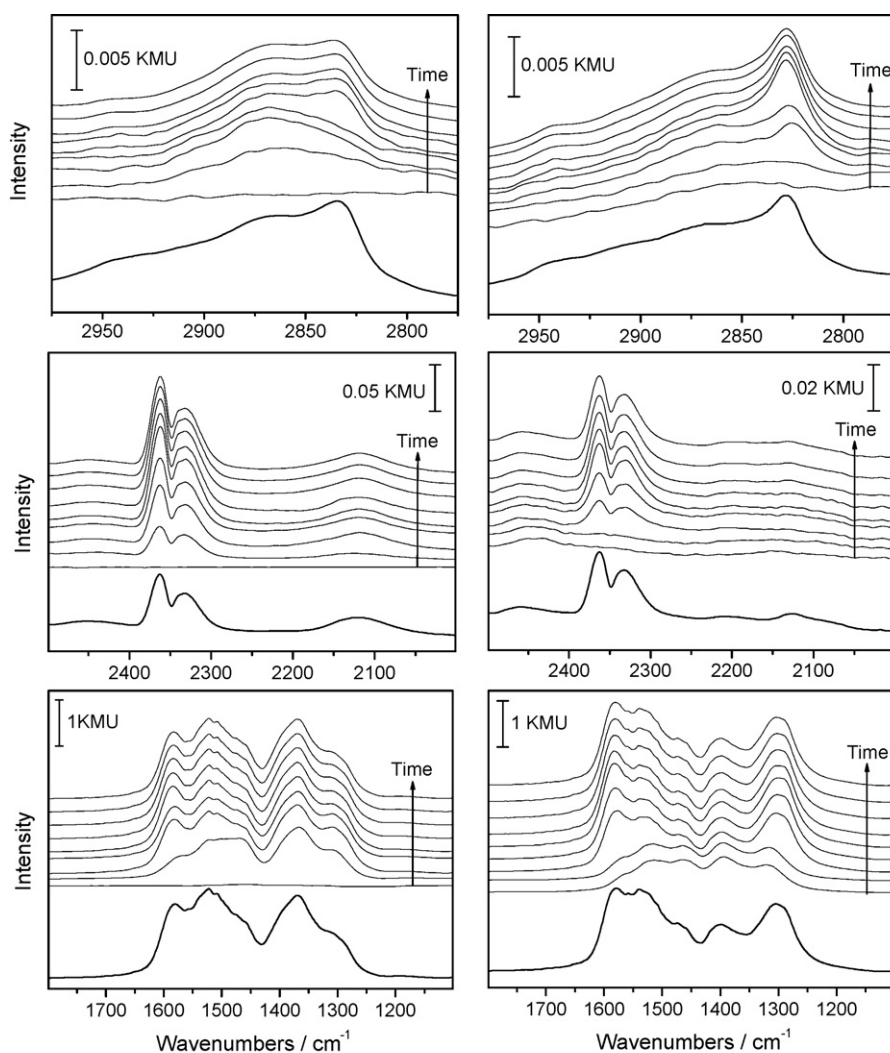
Fig. 7. DRIFT spectra recorded after 1000 min WGS reaction (bold curve) and during WGS reaction (fine curves; reaction times: 0 s, 24 s, 48 s, 1 min, 5 min, 10 min, 30 min, 60 min, 180 min) after reactivation in oxidative atmosphere (O400, left panel) and in reductive atmosphere (H400, right panel) on a 4.5 wt.% Au/CeO$_2$ catalyst in idealized reformate at 300 °C. The following vibrational regions are displayed from bottom to top: OCO region, CO/CO$_2$ region and C–H region.

formation of carbonate species, which blocks active sites for WGS reaction [22], in agreement with recent results for reaction at 180 °C [15,16].

In total, these results convincingly demonstrate that also at 300 °C reaction temperature the deactivation of Au/CeO$_2$ catalysts during the WGS reaction in idealized reformate is mainly caused by formation of stable surface carbonates. By comparison with previous assignments, these are identified as monodentate carbonates. These species either block active reaction sites or the access to these sites. Raising the reaction temperature from 180 to 300 °C was not enough to sufficiently activate the thermal decomposition of these surface carbonate species during the reaction, to reach lower steady-state coverages than at 180 °C reaction temperature. Instead, the deactivation is even more pronounced, and also the monodentate carbonate coverage is significantly higher at 300 °C, indicating that the increase in carbonate formation rate with temperature is dominant. For further experiments one should note that carbonate decomposition can be enhanced by oxygen or water, which is not or only in low concentrations present in this reaction mixture. It would be worthwhile to test whether the addition of water, which is present in high concentrations in realistic reformate, and which was also found to reactivate the catalyst in previous reactivation

measurements [19], results in a decreased deactivation at higher reaction temperatures.

4. Conclusion

We have investigated the effect of a higher reaction temperature, 300 °C instead of the previously used 180 °C, on the activity, stability and deactivation behavior of a 4.5 wt.% Au/CeO$_2$ catalyst in the WGS reaction in idealized reformate, evaluating also the influence of different pretreatment procedures. These included (reactive) annealing of the catalyst at 400 °C in inert, oxidative, or reductive atmospheres, or a combination of these in redox procedures. In addition to reaction rate measurements, the surface composition and the nature and abundance of stable adsorbed reaction intermediates and side products were evaluated by *ex situ* XPS and *in situ* DRIFTS spectroscopy. These measurements led to the following conclusions:

1. The increased reaction temperature results in a significant increase of the reaction rate. Temperature dependent measurements in the range 250–350 °C reveal a linear correlation between ln rate and 1/T. This yields apparent activation ener-

gies for reaction of $45 \pm 2 \, \mathrm{kJ \, mol^{-1}}$ after oxidative pretreatment and $50 \pm 2 \, \mathrm{kJ \, mol^{-1}}$ after reductive pretreatment. These values differ slightly from the $40 \pm 2 \, \mathrm{kJ \, mol^{-1}}$ determined previously for reaction at 180 °C under similar reaction conditions (reductive pretreatment). The differences are not sufficient, however, to conclude on a change in dominant reaction pathway, though it cannot be ruled out either. A similar reaction pathway at both temperatures is supported also by DRIFTS measurements, which show the formation of similar reaction intermediates and side products at both reaction temperatures.

2. In contrast to expectations, the deactivation of the Au/CeO_2 catalyst does not decrease with temperature, but instead is more pronounced at 300 °C than observed for reaction at 180 °C.

3. The pretreatment conditions have a considerable effect on the reaction behavior of the Au/CeO_2 catalysts. Oxidative pretreatments lead to the highest activity and highest tendency for deactivation (lowest stability), while for reductive treatment in H_2 this is opposite. This agrees with findings for the activity for reaction at 180 °C on a 2.7 wt.% Au/CeO_2 catalyst, while for the stability the trend is opposite.

4. The pretreatment has significant influence on the nature of the Au species. After reductive pretreatment, the amount of Au^0 nanoparticle is highest (H400: 73%, CO400: 89%) and that of very small $Au^{0'}$ particles and Au^{3+} species is lowest. After oxidative pretreatment, only 35% of the XPS accessible Au is present as Au^0, while the remaining fraction is present as $Au^{0'}$ (45%) or Au^{3+} (20%), respectively. The Ce^{3+} content, in contrast, is only little affected by the different pretreatment conditions.

5. With ongoing reaction, the differences in surface composition (distribution of Au states) become smaller and the catalyst surface develops towards a steady-state situation, which is independent of the pretreatment procedure. Similarly, the differences in activity of the differently pretreated catalysts become smaller with time on stream.

6. For all catalysts, the deactivation is mainly related to the formation of stable monodentate surface carbonates during the WGS reaction at 300 °C, similar to previous findings for reaction at 180 °C. Effects from sintering of the Au nanoparticles or overreduction of the support are small or negligible, respectively. The surface carbonates either block the active sites for reaction, e.g., for the formation and/or decomposition of the reaction intermediate, or they block the access of these intermediates to the active sites.

7. In contrast to reductive reactivation, re-conditioning in O_2 at 400 °C regains 95% of the initial activity observed on the freshly conditioned catalyst after 1000 min reaction at 300 °C. IR data show, that this is accompanied by complete removal of all surface carbonates and formates. Reductive reconditioning at 400 °C, on the other hand, has little effect on the activity, and monodentate surface carbonates are only reduced in coverage, while formates and bidentate surface carbonates are also removed. This supports the above identification of monodentate surface carbonate species as main origin for catalysts deactivation during the WGS reaction also at 300 °C reaction temperature. The Au^{3+} and $Au^{0'}$ contents also increased during calcination, but remained clearly below their initial values on the freshly conditioned catalyst. This leaves an assignment of these species as rate limiting active species and deactivation due to their decreasing availability less probable.

Acknowledgement

References

[1] D.L. Trimm, Z.I. Önsan, Catal. Rev. 43 (2001) 31.
[2] S. Gottesfeld, T.A. Zawodzinski, in: R.C. Alkire, H. Gerischer, D.M. Kolb, C.W. Tobias (Eds.), Advances in Electrochemical Science and Engineering, vol. 5, Wiley-VCH, Weinheim, 1997.
[3] S. Kawatsu, J. Power Sources 71 (1998) 150.
[4] B.A. Peppley, J.C. Amphlett, R.F. Mann, in: W. Vielstich, A. Lamm, H.A. Gasteiger (Eds.), Fuel Cells and Technology, Handbook of Fuel Cells—Fundamentals Technology and Applications, vol. 3, Wiley, Chichester, 2003.
[5] K. Kochloefl, in: G. Ertl, H. Knözinger, J. Weitkamp (Eds.), Handbook of Heterogeneous Catalysis, vol. 2, Wiley-VCH, Weinheim, 1997.
[6] T. Bunluesin, R.J. Gorte, G.W. Graham, Appl. Catal. B 15 (1998) 107.
[7] Y. Li, Q. Fu, M. Flytzani-Stephanopoulos, Appl. Catal. B 27 (2000) 179.
[8] Q. Fu, H. Saltsburg, M. Flytzani-Stephanopoulos, Science 301 (2003) 935.
[9] T. Luo, J.M. Vohs, R.J. Gorte, J. Catal. 210 (2002) 397.
[10] D. Andreeva, Gold Bull. 35 (2002) 82.
[11] A. Goguet, R. Burch, Y. Chen, C. Hardacre, P. Hu, R.W. Joyner, F. Meunier, B.S. Mun, D. Thompsett, D. Tibiletti, J. Phys. Chem. C 111 (2007) 16927.
[12] F. Meunier, D. Reid, A. Goguet, S. Shekhtman, C. Hardacre, R. Burch, W. Deng, M. Flytzani-Stephanopoulos, J. Catal. 247 (2007) 277.
[13] F. Meunier, A. Goguet, R. Burch, D. Thompsett, J. Catal. 252 (2007) 18.
[14] R. Burch, Phys. Chem. Chem. Phys. 8 (2006) 5483.
[15] Y. Denkwitz, A. Karpenko, V. Plzak, R. Leppelt, B. Schumacher, R.J. Behm, J. Catal. 246 (2007) 74.
[16] A. Karpenko, Y. Denkwitz, V. Plzak, J. Cai, R. Leppelt, B. Schumacher, R.J. Behm, Catal. Lett. 116 (2007) 106.
[17] A. Karpenko, R. Leppelt, V. Plzak, J. Cai, A. Chuvilin, B. Schumacher, U. Kaiser, R.J. Behm, Top. Catal. 44 (2007) 183.
[18] A. Karpenko, R. Leppelt, V. Plzak, R.J. Behm, J. Catal. 252 (2007) 231.
[19] A. Karpenko, R. Leppelt, J. Cai, V. Plzak, A. Chuvilin, U. Kaiser, R.J. Behm, J. Catal. 250 (2006) 139.
[20] A. Karpenko, D. Widmann, R. Leppelt, R.J. Behm, submitted for publication.
[21] R. Leppelt, B. Schumacher, V. Plzak, M. Kinne, R.J. Behm, J. Catal. 244 (2006) 137.
[22] C.H. Kim, L.T. Thompson, J. Catal. 230 (2005) 66.
[23] X. Liu, W. Reuttinger, X. Xu, R. Farrouto, Appl. Catal. B 56 (2005) 69.
[24] S. Hilaire, X. Wang, T. Luo, R.J. Gorte, J. Wagner, Appl. Catal. A 258 (2004) 271.
[25] V. Plzak, J. Garche, R.J. Behm, Eur. Fuel Cell News 10 (2003) 16.
[26] M. Romeo, K. Bak, J. El Fallah, F. Le Normand, L. Hilaire, Surf. Interface Anal. 20 (1993) 508.
[27] D. Briggs, M.P. Seah, Practical Surface Analysis—Auger and X-Ray Photoelectron Spectroscopy, second ed., John Wiley & Sons, Chichester, 1990.
[28] M.J. Kahlich, H.A. Gasteiger, R.J. Behm, J. Catal. 171 (1997) 93.
[29] I.M. Hamadeh, P.R. Griffiths, Appl. Spectrosc. 41 (1987) 682.
[30] J. Sirita, S. Phanichphant, F.C. Meunier, Anal. Chem. 79 (2007) 3912.
[31] Q. Fu, W. Deng, H. Saltsburg, M. Flytzani-Stephanopoulos, Appl. Catal. B 56 (2005) 57.
[32] Q. Fu, A. Weber, M. Flytzani-Stephanopoulos, Catal. Lett. 77 (2001) 87.
[33] D. Andreeva, V. Idakiev, T. Tabakova, L. Ilieva, P. Falaras, A. Bourlinos, A. Travlos, Catal. Today 72 (2002) 51.
[34] A. Luengnaruemitchai, S. Osuwan, E. Gulari, Catal. Commun. 4 (2003) 215.
[35] J.M. Zalc, V. Sokolovskii, D.G. Loeffler, J. Catal. 206 (2002) 169.
[36] D. Tibiletti, F.C. Meunier, A. Goguet, D. Reid, R. Burch, M. Boaro, M. Vicario, A. Trovarelli, J. Catal. 244 (2008) 183.
[37] R. Holm, S. Storp, Appl. Phys. 9 (1976) 217.
[38] J.-J. Pireaux, M. Liehr, P.A. Thiry, J.P. Delrue, R. Caudano, Surf. Sci. 141 (1984) 221.
[39] J.F. Moulder, W.F. Stickle, P.E. Sobol, K.D. Bomben, Handbook of X-ray Photoelectron Spectroscopy, PerkinElmer Corp., Eden Prairie/USA, 1992.
[40] Y. Denkwitz, Z. Zhao, U. Hörmann, U. Kaiser, V. Plzak, R.J. Behm, J. Catal. 251 (2007) 363.
[41] G.K. Wertheim, S.B. DiCenzo, S.E. Youngquist, Phys. Rev. Lett. 51 (1983) 2310.
[42] M. Haruta, S. Tsubota, T. Kobayashi, H. Kageyama, M.J. Genet, B. Delmon, J. Catal. 144 (1993) 175.
[43] H.-G. Boyen, A. Ethirajan, G. Kästle, F. Weigl, P. Ziemann, G. Schmid, M.G. Garnier, M. Büttner, P. Oelhafen, Phys. Rev. Lett. 94 (2005) 016804.
[44] A. Laachir, V. Perrichon, A. Badri, J. Lamotte, E. Catherine, J.C. Lavalley, J. Chem. Soc. Faraday Trans. 87 (1991) 1601.
[45] T. Shido, Y. Iwasawa, J. Catal. 136 (1992) 493.
[46] G. Jacobs, P.M. Patterson, L. Williams, E. Chenu, D. Sparks, G. Thomas, B.H. Davis, Appl. Catal. A 262 (2004) 177.
[47] C. Li, Y. Sakata, T. Arai, K. Domen, K. Maruya, T. Onishi, J. Chem. Soc. Faraday Trans. 85 (1989) 1451.
[48] T. Mokkelbost, I. Kaus, T. Grande, M.A. Einarsrud, Chem. Mater. 16 (2004) 5489.
[49] A. Bumajdad, M.I. Zaki, J. Eastoe, L. Pasupulety, Langmuir 20 (2004) 11223.
[50] F. Bozon-Verduraz, A. Bensalem, J. Chem. Soc. Faraday Trans. 90 (1994) 653.
[51] C. Binet, M. Daturi, J.-C. Lavalley, Catal. Today 50 (1999) 207.
[52] C. Li, Y. Sakata, T. Arai, K. Domen, K. Maruya, T. Onishi, J. Chem. Soc. Faraday Trans. 85 (1989) 929.
[53] C. Binet, A. Badri, J.C. Lavalley, J. Phys. Chem. 98 (1994) 6392.
[54] E. Finocchio, M. Daturi, C. Binet, J.C. Lavalley, G. Blanchard, Catal. Today 52 (1999) 53.
[55] T. Tabakova, F. Boccuzzi, M. Manzoli, D. Andreeva, Appl. Catal. A 252 (2003) 385.
[56] M. Manzoli, F. Boccuzzi, A. Chiorino, F. Vindigni, W. Deng, M. Flytzani-Stephanopoulos, J. Catal. 245 (2007) 308.
[57] A. Holmgren, B. Andersson, D. Duprez, Appl. Catal. B 22 (1999) 215.

[58] F. Boccuzzi, A. Chiorini, Stud. Surf. Sci. Catal. 140 (2001) 77.
[59] T. Shido, Y. Iwasawa, J. Catal. 141 (1993) 71.
[60] A.M. Bradshaw, J. Pritchard, Proc. R. Soc. A 316 (1970) 169.
[61] J. France, P. Hollins, J. Electron Spectrosc. Relat. Phenom. 64/65 (1993) 251.

[62] F. Boccuzzi, A. Chiorini, M. Manzoli, P. Lu, T. Akita, S. Ichikawa, M. Haruta, J. Catal. 202 (2001) 256.
[63] V. Shapovalov, H. Metiu, J. Catal. 245 (2007) 205.
[64] D. Widmann, R. Leppelt, R.J. Behm, J. Catal. 251 (2007) 437.